THE JOURNAL OF PHYSICAL CHEMISTRY B

Article

pubs.acs.org/JPCB

Influence of Chemical Structure on Hydration and Gas Transport Mechanisms of Sulfonated Poly(aryl ether ketone) Membranes

Sandra Simon,[†] Eliane Espuche,*[,†] Fabrice Gouanvé,[†] Edouard Chauveau,[‡] Catherine Marestin,[‡] and Régis Mercier[‡]

[†]Université de Lyon, Université Lyon 1, CNRS, UMR 5223, Ingénierie des Matériaux Polymères, Bât. POLYTECH, 15 Bd A. Latarjet, 69622 Villeurbanne Cedex, France

[‡]LEPMI - UMR 5279 - CNRS/INP Grenoble/UJF/Université de Savoie, Chemin du Canal, 69 360 Solaize, France

ABSTRACT: This work reports the influence of the chemical structure of two sulfonated poly(aryl ether ketone)s (SPAEK) on the hydration and gas transport mechanism of thin membranes made thereupon. For this purpose, two sulfonated poly(aryl ether ketone)s having the same ionic exchange capacity (IEC) but bearing a different repartition of the sulfonic acid groups along the polymer backbone were prepared. These polymers were synthesized by direct copolymerization of two specific sulfonated precursors, bisphenol AF and 4,4′-difluorobenzophenone. The morphology of the membranes was studied by transmission electron microscopy, and the thermal properties of the ionomers were determined from differential scanning calorimetry and thermogravimetric analyses. A detailed analysis of the water sorption isotherms and kinetics was performed. The gas transport properties were also determined for He, H_2, and CO_2 in the full range of water activity. From the detailed analysis of the water sorption isotherm and of the relative contributions of the Fickian diffusion and relaxation phenomena, a water sorption mechanism was proposed in relation with the SPAEK architectures and polymers' chain mobility. This mechanism allowed explaining the different evolution of the gas transport properties observed as a function of the gas nature and hydration rate.

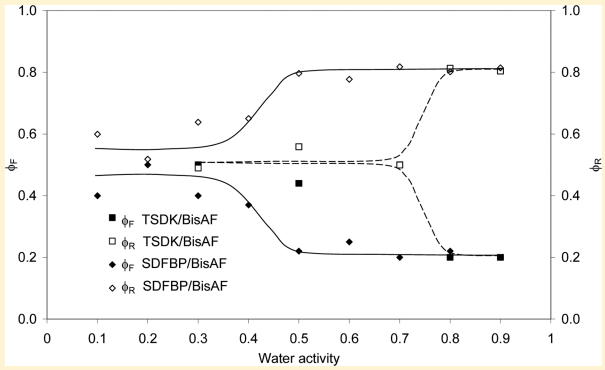

1. INTRODUCTION

Proton exchange membrane fuel cells (PEMFCs) have emerged as alternative energy devices for a wide range of applications covering portable and mobile applications in transportation and domestic power pack. In the polymer electrolyte membrane fuel cell, the polymer electrolyte membrane (PEM) has a key role as it has to provide the ionic pathway, keeping good mechanical and gas barrier properties all along the fuel cell working life. The water sorption and diffusion mechanisms in the membrane are also determining factors for optimized fuel cell working performance. Indeed, water enters the membrane either from humidified feeds or from water generated at the cathode, and it is important to control the distribution of water throughout the fuel cell especially for the local proton conductivity.

Perfluorosulfonic acid membranes, such as Nafion, have been extensively studied as proton exchange membranes. These membranes have high proton conductivity and good chemical and mechanical stability. However, Nafion membranes present some limitations. They are expensive, they highly swell and plasticize upon water exposure, and they cannot operate at temperatures higher than 80 °C due to the strong reduction of proton conductivity related to dehumidification problems.[1−3]

Different routes have been investigated in order to synthesize new polymer-based materials as possible alternative to Nafion. One particularly interesting way has consisted in preparing sulfonated high performance polymers. Among the different materials derived from this approach (sulfonated polyimides, sulfonated poly(ether sulfone)s, etc.)[4−7] sulfonated poly(ether ether ketones) (SPEEK) have attracted considerable attention.[8−12] Depending on their sulfonation degree, SPEEK can be, contrary to pristine PEEK, amorphous and soluble in many organic solvents, which makes them suitable for the preparation of membranes by casting process. Sulfonated PEEK exhibits obvious differences in phase separation behavior and morphology from Nafion.[13,14] Hydrophilic/hydrophobic phase separation is less distinctive due to a less hydrophobic character of the backbone PEEK chains in comparison with Nafion fluorinated backbone. The degree of sulfonation which controls, to a large part, the hydrophobic−hydrophilic balance and then a variety of properties, such as thermal and mechanical properties or proton conductivity, can be varied in a wide range by means of different routes. SPEEK has often been prepared by postsulfonation of the commercially available high-performance PEEK polymer backbone in different reaction media (concentrated sulfuric acid, chlorosulfonic

Received: June 6, 2012
Revised: August 30, 2012
Published: October 12, 2012

acid, or methanesulfonic acid).[8,10,11,15−19] However, by this route, the introduction of the sulfonic acid groups is usually restricted to the position ortho to the aromatic ether bond, and the degree of sulfonation can be hard to control with the risk, for high sulfonation degrees, to deteriorate more rapidly the polymer mechanical properties and long-term stability. Moreover, the postmodification reaction can be performed in heterogeneous or homogeneous media and then lead to different and not always well-controlled copolymer architectures.[11] An alternative to the postsulfonation route has consisted in preparing sulfonated poly(ether ether ketone) or more generally sulfonated poly(aryl ether ketone)s (SPAEK) by direct copolymerization of sulfonated monomers. By this way, a wide variety of structures can be obtained.[12,20−28] Whereas few polymers have been synthesized from sulfonated bisphenols,[21−26] the sulfonic acid groups are mainly introduced in the polymer backbone chain by condensation of sulfonated difluorobenzophenone and different nonsulfonated bisphenols.[27,28] The functional properties of the resulting sulfonated copolymers are of course related to the sulfonation degree that can be easily tailored but they can also result from the state of aggregation of polymer chain segments, which depends in a great part on the different structures of repeat units in polymer chains. Some authors have also underlined a significant influence of the repartition of the sulfonated groups along the polymer backbone on specific functional properties such as proton conductivity, by changing the respective hydrophobic and hydrophilic polymer block lengths.[12,23,29,30] However, such relationships were never studied considering other SPAEK functional properties, namely gas transport and water hydration properties, or other routes allowing to vary the sulfonic acid group repartition.

The objective of this work is to investigate the relationships between the sulfonic acid groups repartition in a PAEK backbone and the hydration and gas transport mechanisms which are important features for optimized fuel cell working properties and to propose a transport model for these materials. In this study, the copolymerization route is chosen to perfectly control the copolymer structure, and a new sulfonated monomer, namely a highly sulfonated bisdiketone, is designed and used as a new and original mean to vary the sulfonic acid group repartition along the polymer backbone. The use of this monomer in SPAEK synthesis is expected to induce a higher phase separation in the resulting polymer than in SPAEK based on the commonly used sulfonated 4,4′-difluorobenzophenone, which represents the reference material of this study.

2. EXPERIMENTAL PART

2.1. Materials. 4,4′-Hexafluoroisopropylidene diphenol (Bisphenol AF: BisAF) was purified by sublimation, and 4,4′-difluorobenzophenone (DFBP) was purified by crystallization in a petroleum ether/ethyl acetate mixture. *N*-Methylpyrrolidinone (NMP), dimethyl sulfoxide (DMSO), potassium carbonate (K_2CO_3), diphenyl ether, 4-fluorobenzoyl chloride, and fuming sulfuric acid (60% SO_3) were used as received.

2.2. Sulfonated Monomer Characterization. NMR spectra were recorded on a Bruker AC250 spectrometer operating at a resonance frequency of 250.13 MHz for ^{1}H, 62.89 MHz for ^{13}C, and 235 MHz for ^{19}F. Sample solutions were prepared in deuterated DMSO (DMSO-d_6). Tetramethylsilane (TMS) was used as internal reference standard for ^{1}H and ^{13}C; fluorotrichloromethane (FCl_3C) was used as internal reference for ^{19}F measurements.

2.3. SPAEK Synthesis. Typically, in a 150 mL three-necked round-bottom flask equipped with a nitrogen inlet, a mechanical stirrer, and a Dean-Stark trap, 16.15 g of 4,4′-hexafluoroisopropylidene diphenol (48 mmol), 14.59 g of K_2CO_3 (105 mmol), 7.76 g of 4,4′-difluorobenzophenone (35.6 mmol), and 10 g (12.4 mmol) of tetrasulfonated bisdiketone (**2**) were refluxed for 4 h in a mixture of 79 mL of DMSO and 15 mL of toluene. The water released during the bisphenate formation was stripped off by azeotropic distillation with toluene. The temperature was then increased up to 170 °C in order to complete the polymerization (10 h). After cooling, the mixture was poured into methanol. The fiber-like polymer was chucked into pieces and then collected by filtration, washed with methanol, and dried under vacuum at 80 °C for further characterization.

2.4. Membrane Preparation. 15−20 wt % solutions in NMP of the sulfonated polymers in their salt form were filtered (10 μm filter) and cast onto a glass plate. The resulting membranes were successively dried at 50 °C overnight and then 1 h at 80 °C, 1 h at 120 °C, 1 h at 150 °C, and finally 180 °C for 2 h. Dried membranes were peeled off from the substrate by immersion in water. The sulfonated PAEK in their acidic form were obtained by immersing overnight the potassium salt films in 2 M H_2SO_4, at room temperature. The membranes were then rinsed several times with deionized water in order to remove any free H_2SO_4. The membrane thickness was 100 μm.

2.5. Thermogravimetric Analysis (TGA). Thermogravimetric analyses were performed with a TGA 2950-TA Instruments (Guyancourt, France) under a dry helium atmosphere at a heating rate of 10 °C/min from 30 to 800 °C.

2.6. Differential Scanning Calorimetry (DSC). Differential scanning calorimetry (DSC) analysis was performed with a TA Instruments 2920 apparatus under a helium atmosphere at a scanning rate of 10 °C/min from 0 to 250 °C. Two scans were successively recorded with rapid intermediate cooling (50 °C/min). The glass transition temperature was determined from the second scan in order to avoid any plasticization effect due to the presence of water within the film. The glass transition temperature was taken at the mid point of the ΔC_p variation.

2.7. Transmission Electron Microscopy Analysis (TEM). In order to clearly evidence the size and shape of the hydrophilic domains, the SPAEK membranes in their acidic form were treated with a 1 M aqueous $AgNO_3$ solution for 24 h and thoroughly rinsed with deionized water. The stained sPAEK membranes were then embedded in an epoxy resin and microtomed in cross section. The resulting 70−80 nm thick samples were analyzed by TEM, with a Philips CM120 microscope operating at 80 kV.

2.8. Water Vapor Sorption. A dynamic vapor sorption analyzer, DVS Advantage (Surface Measurement Systems Ltd., London, UK), was used to determine the film water sorption properties. The experiments were carried out at 25 °C. The samples (50 mg) were introduced in the microbalance and predried by exposure to dry nitrogen until the dry weight of the samples was obtained. A partial pressure of water was established within the apparatus by mixing dry and water saturated nitrogen. The sample water uptake was followed as a function of time, and the equilibrium was considered to be reached when changes in mass with time (dm/dt) were lower than 0.0002 for 5 consecutive minutes. The partial pressure was then incremented by successive steps, allowing obtaining in all

Scheme 1. Synthesis of Sulfonic Acid Containing Monomers by Direct Sulfonation of Precursors in Fuming Sulfuric Acid

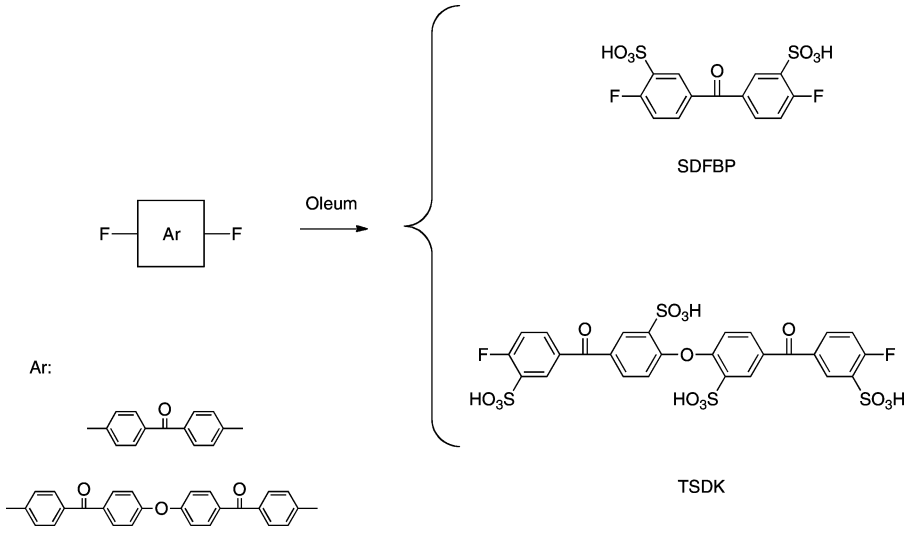

Scheme 2. Synthesis Scheme of TSDK/Bis AF by Aromatic Nucleophilic Substitution

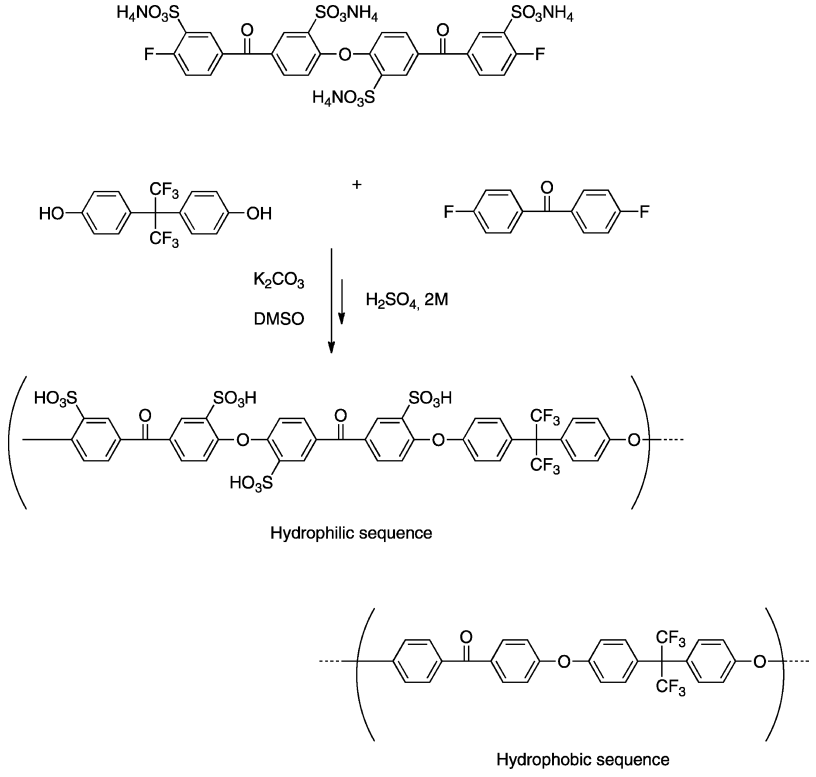

the range of partial pressures the kinetics of water sorption and the sorption isotherm.

For each partial pressure increment, the thermal changes associated with the water uptake were recorded. The peak was integrated and corrected with values of energy obtained under the same conditions with empty boats. The ratio of the obtained energy to the water uptake gave the interaction enthalpy in kJ mol^{-1}. It was representative of the internal enthalpy change of one molecule from gaseous to sorbed state.

2.9. Gas Permeation at Different Relative Humidities. The permeation cell consisted in two compartments separated by the studied membrane. The cell was thermostated at 20 ± 1 °C. A preliminary high-vacuum desorption was realized to ensure that the static vacuum pressure changes in the downstream compartment were smaller than the pressure changes due to the gas diffusion.

For gas permeation at anhydrous state, a 3×10^5 Pa gas pressure was introduced in the upstream. The pressure variations in the downstream compartment were measured with a datametrics pressure sensor. A steady-state line was obtained after a transitory state by plotting the measured pressure versus time. The permeability coefficient expressed in barrer units (1 barrer: 10^{-10} cm^3_{STP} cm cm^{-2} s^{-1} cm_{Hg}^{-1}) was calculated from the slope of the steady-state line. The diffusion coefficient was calculated from the time lag value, determined from the extrapolation of the steady-state line on the time axis.

dx.doi.org/10.1021/jp305541y | J. Phys. Chem. B 2012, 116, 12750−12759

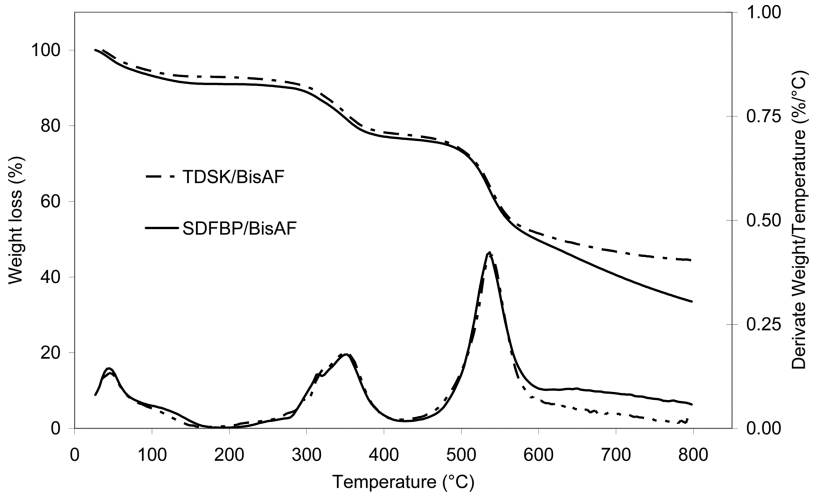

Figure 1. TGA thermograms of (—) SDFBP/BisAF and (- - -) TSDK/BisAF.

For gas permeation experiments at hydrated state, the membrane was equilibrated at the desired water relative partial pressure within the permeation cell before introducing in the upstream compartment the 3×10^5 Pa gas pressure. The permeability coefficient was calculated, as in the previous case, from the data recorded in the steady state. The diffusion coefficient could not be determined in this case.

The results were the average of three different experiments, and the uncertainty on the transport parameters was better than 4% for the permeability coefficients and 8% for the diffusion coefficients.

3. RESULTS AND DISCUSSION

3.1. SPAEK Synthesis. The two sulfonated monomers (sulfonated difluorobenzophenone, SDFBP, and tetrasulfonated diketone, TSDK) synthesized in this work were prepared by direct sulfonation of precursors in fuming sulfuric acid, according to the procedure described by Wang.[27] As reported elsewhere and illustrated in Scheme 1, when the sulfonation of bis(4-fluorobenzoyl)-4,4′-diphenyl ether is performed at high temperature (120 °C), four sulfonic acid groups can be incorporated. Both sodium salts and ammonium salts can be isolated as polymer grade monomers, characterized by NMR, and involved in polycondensation reaction in order to obtain high molecular weight sulfonated poly(aryl ether ketone)s.

4,4′-Difluoro-3,3′-disodium Sulfonate Benzophenone. ^{1}H NMR (DMSO-d_6, RT): δ (ppm) = 7.35 (dd, H^5, $J_{5,F}$ = 8.8 Hz), 7.74 (m, H^6), 8.06 ppm (dd, H^2, J = 2.3 Hz). ^{13}C NMR (DMSO-d_6, RT): 116.8 (d, C, J = 23.1 Hz), 130.7 (d, C, J = 4.6 Hz), 132.6 (d, C, J = 3.7 Hz), 133.1 (d, C, J = 9.2 Hz), 135.6 (d, C, J = 17.6 Hz), 161.4 (d, C, J = 257.1 Hz), 193.2 (C═O). ^{19}F NMR (DMSO-d_6, RT): δ (ppm) = −104.8.

Bis(3-ammonium-4-fluorobenzoyl)-4,4′-di(2-ammonium sulfonate phenyl ether). ^{1}H NMR (DMSO-d_6, 370 K): δ (ppm) = 7.01 (d, $J_{5,6}$ = 8.4 Hz), 7.37 (dd, $J_{11,F}$ = 8.9 Hz), 7.77 (m), 8.1 (dd, $J_{3,5}$ = 2.3 Hz, $J_{5,6}$ = 4.8 Hz), 8.2 (d, $J_{3,5}$ = 2.3). ^{13}C NMR (DMSO-d_6, RT): 116 (d, 23.1 Hz), 120, 129.8, 130.1, 130.2 (d, J = 4.4 Hz), 131.8, 131.9, 132.5 (d, J = 3.7 Hz), 135.6 (d, J = 17.54 Hz), 138, 156.5, 160.8 (d, J = 257.1 Hz), 192.7 (C═O). ^{19}F NMR (DMSO-d_6, RT): δ (ppm) = −104.7.

In order to check the effect of the sulfonic acid repartition along the polymer backbone on the final polymer properties, this work focuses on the comparison of two different kinds of sulfonated polyarylether ketones (SPAEK) bearing the same ionic exchange capacity (namely 1.6 mequiv H^+/g). The first macromolecular structure (SDFBP/BisAF) is based on the disulfonated benzophenone, whereas the second ionomer (TSDK/BisAF) contains the tetrasulfonated bisdiketone. In both cases, the comonomers used in this work were bisphenol AF and difluorobenzophenone (Scheme 2). Both polymers were soluble in common organic solvents. Thin defect-free membranes were cast from NMP solutions, and the acidic forms of the sulfonic acid groups were regenerated by immersing the thin membranes in 2 M sulfuric acid solutions.

3.2. SPAEK Membrane Characterization. The degradation process and the thermal stability of the membranes were investigated by thermal gravimetry analysis. The two membranes exhibited similar weight loss curves (Figure 1).

The weight loss observed below 150 °C can be assigned to water desorption from the polymer film. Indeed, this weight loss corresponds exactly to the water uptake determined by sorption measurements in ambient conditions. A two-step degradation mechanism was evidenced at higher temperatures. The first weight loss observed between 270 and 400 °C can be associated with the decomposition of sulfonic groups.[12,20,31] The second weight loss step at around 536 °C reflects the degradation of the main chain of SPAEK. The experimental IEC value was calculated from the weight loss step at temperatures ranging between 200 and 400 °C, assuming that this weight loss is entirely due to $-SO_3H$ release. The calculation was performed by considering the weight of dry material. It led to an IEC experimental value of 1.66 mequiv g^{-1}, which is in good agreement with the theoretical one, 1.60 mequiv g^{-1}.

The DSC second heating curves, from which the SPAEK glass transition values were determined, are presented in Figure 2. As expected, the SPAEK films are totally amorphous. The values of the SPAEK glass transition temperature are reported in Figure 3 and compared to the T_g values given in the literature for SPEEK of different IEC values.[11,32,33]

A good agreement is observed between all the data, with a shift of T_g toward higher temperatures with increasing IEC values. This trend is generally explained by increased intermolecular interactions by hydrogen bonding of SO_3H groups and increased molecular bulkiness that hinder the internal rotations compared to unsulfonated PEEK.[34] However,

dx.doi.org/10.1021/jp305541y | J. Phys. Chem. B 2012, 116, 12750−12759

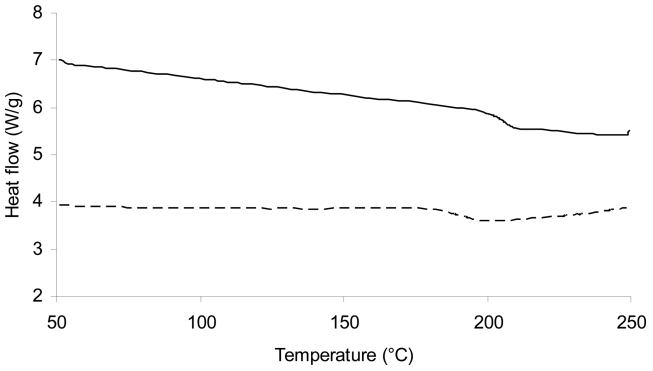

Figure 2. DSC second heating scan performed on (—) SDFBP/BisAF and (- - -) TSDK/BisAF.

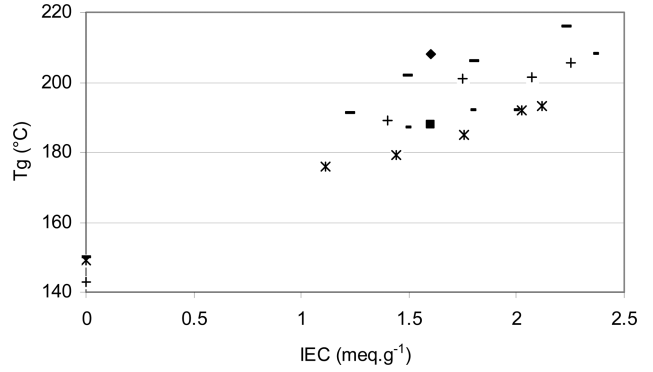

Figure 3. Comparison between the glass transition temperature values of the two SPEEK films ((■) TSDK/BisAF, (◆) SDFBP/BisAF) with respect to those reported for other SPEEKs in the literature ((-) homogeneous sulfonation Do et al.,[11] (+) heterogeneous sulfonation Do et al.,[11] (∗) Shashidhara et al.,[32] (−) Wilhelm et al.[33]).

SDFBP/BisAF displays a significantly higher T_g value than TSDK/BisAF (208 and 188 °C, respectively) despite an identical IEC value and totally similar polymer synthesis and film forming conditions. This result shows that the polymer chain mobility can be tailored in a significant extent by the control of the repartition of the sulfonated groups all along the polymer backbone chain. The use of SDFBP should lead to a more homogeneous repartition of the ionic groups and hydrophilic domains within the materials and then contribute to hinder to a higher extent the chain mobility. In order to have more information on the ionic group organization at a nanoscopic scale, a TEM analysis was performed.

Some authors[23,35,36] identified the presence of various domains which they attribute to hydrophilic and hydrophobic regions using atomic force microscopy or transmission electron microscopy. Analyzing different samples of given chemical structures but with increasing IEC, an increase of the hydrophilic domain size with the amount of sulfonic groups is typically reported. In such experiments, the sulfonated groups have to be preliminary stained (by either silver or lead ions) in order to have a good contrast between the different membrane regions and therefore better identify the hydrophilic domains.

However, most TEM observations reported were done on thin films made out of stained SPEEK solutions directly cast onto TEM copper grid[37,38] or even on stained SPEEK powders.[39] As the experimental conditions are supposed to have a strong influence on the final morphology of the membranes, the characterization of thin films elaborated either in their Ag^+ or Pb^{2+} form is suspected to be not rigorously representative of the morphology of a typical proton exchange membrane.

For that reason, the samples analyzed in this study were SPAEK membranes in their acidic form which were embedded in an epoxy resin after staining the hydrophilic domains by $AgNO_3$. The membranes were cutted in their cross section before TEM analysis. Two TEM images representative of the micrographs obtained on the membranes are presented in Figure 4. For both polymers, the hydrophilic domains are

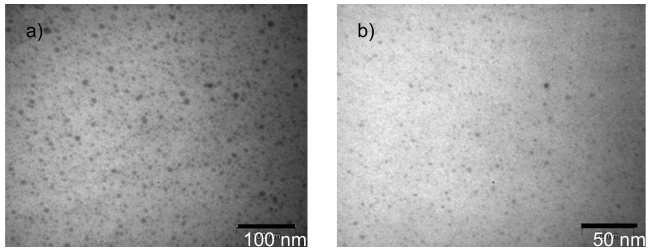

Figure 4. TEM analysis: (a) TSDK/BisAF and (b) SDFBP/BisAF.

discrete, spherical regions, uniformly dispersed in the hydrophobic matrix. As shown in Figure 4, it seems that the polymer comprising the tetrasulfonated monomer presents larger hydrophilic domains (diameter ∼8 nm) than its analogue based on the sulfonated benzophenone (diameter ∼4 nm). This observation is not surprising as the incorporation of the tetrasulfonated monomer induces locally a high concentration of sulfonic groups. At a nanoscopic scale, it could thus favor the formation of larger hydrophilic clusters.

Hydration properties are one of the challenging properties for polymer electrolyte membrane fuel cell working properties. However, much experimental research concerned with SPEEK or SPAEK only consisted in determining the water uptake of the polymer immersed in liquid water, considering different IEC.[11,20] Only few works dealt with the detailed investigation of the water hydration mechanism, considering both thermodynamic and kinetic behaviors in all the range of activity. Moreover, these studies were only focused on SPEEK prepared from postsulfonation route.[14,40]

The objective of the present work is to see if TSDK/BisAF, which exhibits, for the same IEC value than SDFBP/BisAF, a different repartition and nanoscale organization of the sulfonated groups as well as a different polymer chain mobility, displays also different water and gas transport mechanisms.

The water uptakes were determined for the two SPAEK films on all the range of activity. The experimental data defined a single water sorption isotherm curve (Figure 5a) characterized by a sigmoidal shape. This shape, which is typical of BET II isotherm in the classification of Brunauer−Emmett−Teller, shows three distinct parts: The first part, observed at low activity, presents a concave form which is usually analyzed, for ionomers, as water sorption in primary hydration of the ionic groups. The second part, observed in the range of water activity between 0.3 and 0.6, is linear and corresponds to a Henry sorption mode. The last part, exhibiting a convex form, is related to water clustering. The sorption data were also represented as the number of water molecules sorbed per sulfonic acid group, denoted as λ (Figure 5b). As underlined by Figure 5b, λ values are in good agreement with the values reported in the literature for different SPEEK membranes prepared from a postsulfonation treatment.[40] The differential

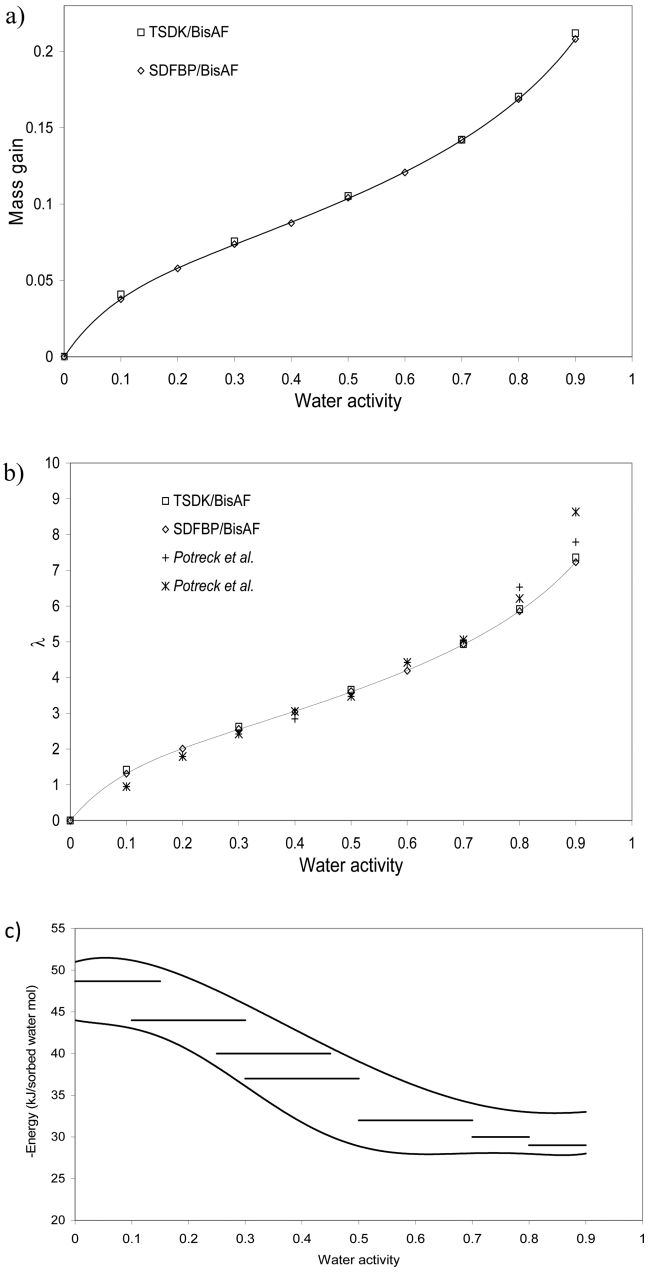

Figure 5. Water sorption isotherm expressed as (a) water uptake as a function of the water activity and (b) number of water molecules sorbed per SO_3H group as a function of the water activity. In this representation, the data obtained on SPEEK prepared by postsulfonation for DS = 59% and 75% were reported,[40] and (c) energy involved in the water sorption mechanism in absolute value.

molar enthalpy of interaction involved in the sorption process was also determined, and its values were reported in Figure 5c. The ΔH profile observed as a function of the water activity is in agreement with the water sorption mechanism with three characteristic domains.[5,41] The confrontation between the curves of Figure 5b,c shows that at low activity two water molecules are strongly interacting with each ionic group. Then, at middle water activity (between 0.2 and 0.6), two additional water molecules are involved in the sorption mechanism and progressively develop a decreasing mean interaction enthalpy in absolute value. At last, at water activity higher than 0.6, the sorption mechanism consists in the formation of water clusters implying a mean interaction enthalpy value that becomes constant and similar to that of water liquefaction. According to this analysis, the water clusters are composed, in each SPAEK material, of 8 water molecules per sulfonic acid group at high activity (near to 0.9), more exactly 4 water molecules surrounding the four first and more highly bonded ones that could form, in agreement with the Wu et al.[14] sorption model developed for SPEEK, the first hydration shell of the sulfonic acid groups. This analysis seems then to underline the prevailing role of the ionic group concentration on the thermodynamic aspects of the water sorption mechanism and the insignificant influence of the repartition of the sulfonated groups on the equilibrium water uptake. It was interesting to see if the same conclusions could be drawn considering water sorption kinetics.

Figure 6a,b shows typical plots of the normalized water vapor uptake, e.g., the water uptake at the time t ratioed to the water uptake at equilibrium, versus the normalized square root of time for the two membranes at the water activity values from 0 to 0.1 and from 0.7 to 0.8, respectively. The same trends are observed for the two membranes: the water sorption mechanism cannot be considered as purely Fickian. Such behavior has already been observed in the literature and has been assigned to Fickian sorption on one hand and relaxational phenomena on the other hand. The linear part of the curves

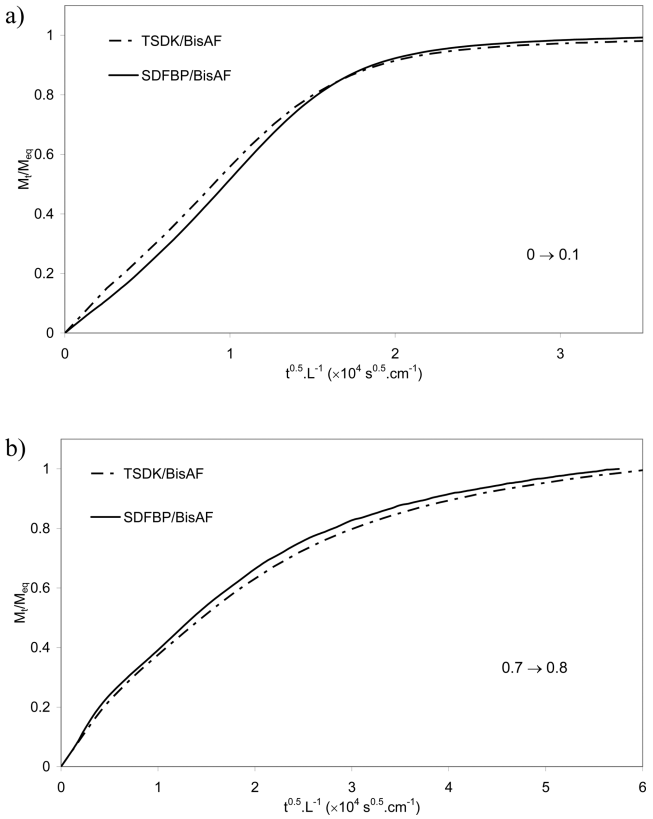

Figure 6. (a) Plots of the normalized water vapor uptake, e.g., the water uptake at the time t ratioed to the water uptake at equilibrium, versus the normalized square root of time at the water activity from 0 to 0.1 for (—) SDFBP/BisAF and (- - -) TSDK/BisAF. (b) Plots of the normalized water vapor uptake, e.g., the water uptake at the time t ratioed to the water uptake at equilibrium, versus the normalized square root of time at the water activity from 0.7 to 0.8 for (—) SDFBP/BisAF and (- - -) TSDK/BisAF.

dx.doi.org/10.1021/jp305541y | J. Phys. Chem. B 2012, 116, 12750−12759

during the initial stage is assigned to the Fickian contribution, whereas the upward curvature that is observed before reaching the equilibrium water uptake ($M_t/M_{eq} = 1$) is representative of the relaxation contribution. The deviation from Fickian law appears as more significant as the water activity increases, and the non-Fickian contribution can be described as a series of relaxational regimes, of which can be characterized by its specific relaxation rate k_R.

The parallel model developed by Hopfenberg–Berens[42] allows taking into account Fickian and relaxational contributions through the equation

$$\frac{M_t}{M_{eq}} = \phi_F\left(1 - \sum_{n=0}^{\infty} \frac{8}{(2n+1)^2\pi^2} \exp\left[-\frac{(2n+1)^2\pi^2 Dt}{L^2}\right]\right) + \sum_{i=1}^{\infty} \phi_{Ri}(1 - \exp[-k_{Ri}t]) \quad (1)$$

$$\phi_F = M_{eq,F}/M_{eq}, \quad \phi_{Ri} = M_{eq,Ri}/M_{eq}, \quad \phi_R = \sum_i \phi_{Ri},$$

$$\phi_F + \phi_R = 1$$

where Φ_F is the weight fraction of vapor sorbed at equilibrium for the Fickian contribution, Φ_{Ri} are the weight fractions of vapor sorbed at equilibrium for the relaxation contribution, and k_{Ri} are their respective relaxation rate constants. In this equation, the first term is the contribution of Fickian diffusion and the second term the contribution due to polymer relaxation. This relaxation contribution is assumed to be first order in the concentration difference which drives the relaxation. The Hopfenberg–Berens model was already successfully used to simulate kinetics sorption of water in SPEEK of different sulfonation degrees obtained by the postsulfonation route.[40] In Potreck's work,[40] the values of the model parameters and their evolution were mainly discussed as a function of the water content within the films. Equation 1 was used in this work to model the experimental kinetics curves of our films with the aim to discuss the role of the sulfonic acid group repartition. An example of fitting, exhibiting the different contributions involved in the modeling, is reported in Figure 7 for SDFBP/BisAF in the activity range from 0.7 to 0.8. The model is convenient and well describes the experimental sorption kinetic curve considering two relaxation contributions.

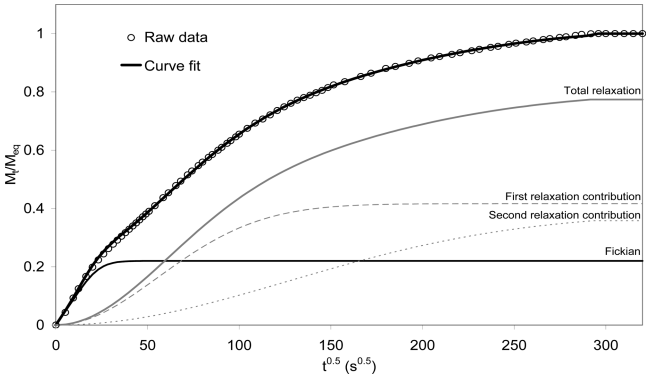

Figure 7. Example of modeling applied to an experimental kinetic sorption curve for SDFBP/BisAF, which exhibits the different contributions involved in the Hopfenberg–Berens equation.

The values of the parameters of the Hopfenberg–Berens model were determined at each water activity for the two SPEEK films. Figure 8a establishes a comparison of the Fickian

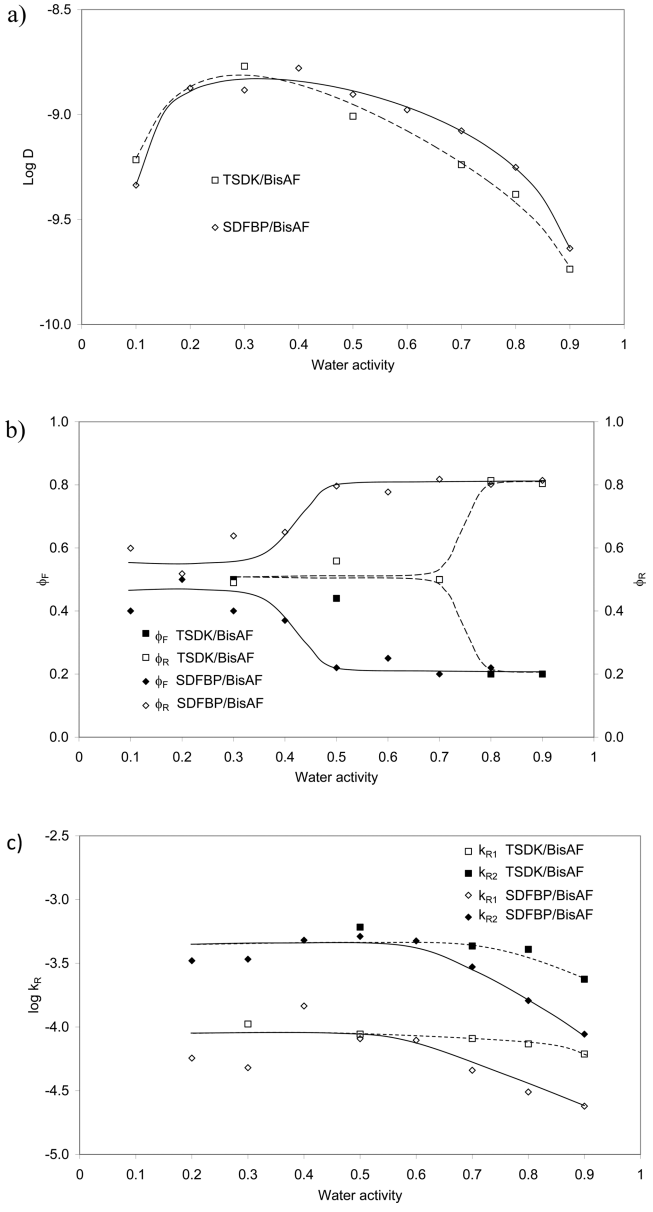

Figure 8. (a) Evolution of the logarithm of the diffusion coefficient (D being expressed in $cm^2\ s^{-1}$) as a function of the water activity for SDFBP/BisAF and TSDK/BisAF. (b) Evolution of the Fickian fraction and of the relaxation fraction induced in the water sorption mechanism as a function of the water activity for (–) SDFBP/BisAF and (- - -) TSDK/BisAF. (c) Evolution of the logarithm of the relaxation rate constants (k_{R1} and k_{R2} being expressed in s^{-1}) as a function of the water activity for (–) SDFBP/BisAF and (- - -) TSDK/BisAF.

diffusion coefficients extracted from the modeling in all the range of activity. The diffusion coefficient values are in the same range for the two membranes. They increase up to a maximum with increasing water vapor activity, then stay constant, and finally decrease at high activity. This trend has already been reported in the literature for hydrophilic materials,[5,41] and it is in agreement with the three consecutive steps of a BET type II sorption mechanism: sorption on specific sites leading to a

dx.doi.org/10.1021/jp305541y | J. Phys. Chem. B 2012, 116, 12750–12759

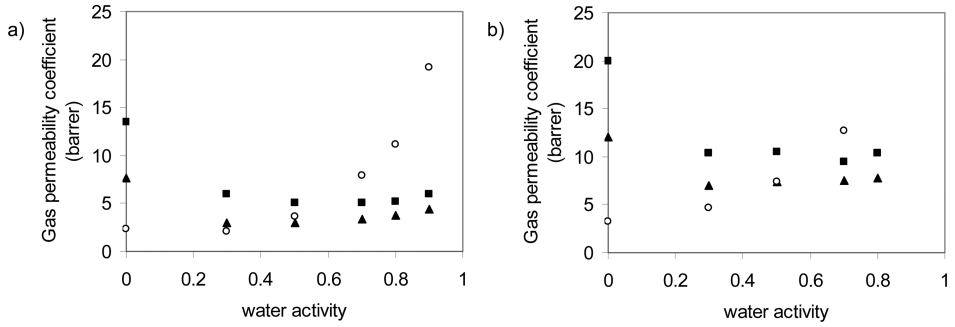

Figure 9. Evolution of (■) helium, (○) carbon dioxide, and (▲) hydrogen permeability coefficients as a function of the water activity for (a) SDFBP/BisAF and (b) TSDK/BisAF.

plasticization effect, Henry contribution accompanied by a constant diffusion, and water cluster formation with a progressive increase of the mean size of the water clusters related to a decrease of the apparent diffusion rate. According to Potreck et al.,[40] the occurrence of the last step, which is clearly observed in our films, depends on the PEEK sulfonation degree. Indeed, the water cluster formation is closely related to the polymer hydrophilicity and to the polymer ability to swell. We have evidenced that the water uptake was governed in SPEEK by the ionic groups (Figure 5b). We can then deduce that the amount of sulfonic groups is high enough in our films to bring the necessary hydrophilicity that promotes this specific behavior.

Figure 8b shows the contribution of Fickian equilibrium sorption (Φ_F) and relaxation equilibrium sorption ($\Phi_R = \Phi_{R1} + \Phi_{R2}$) to the global sorption mechanism in all the range of activity. As the water uptakes at equilibrium are identical for the two membranes, the eventual differences observed between SDFBP/BisAF and TSDK/BisAF will then be directly related to the polymer structure and initial polymer chain mobility. Whatever the membrane, three steps can be evidenced. In the first step Φ_F and Φ_R stay constant. In this step, the values of Φ_F and Φ_R are similar for the two membranes and rather identical (near to 0.5 for each one). The intermediate step is characterized by a decrease of the Fickian contribution and in the meantime by an increase of the relaxation contribution. In the last step, the two contributions reach a plateau value. Here again, the values of Φ_F and Φ_R are similar for the two membranes, close to 0.2 and 0.8, respectively. The main difference observed between the two membranes is that the first step is restricted to the range of activity below 0.3 for SDFBP/BisAF, whereas it concerns a wider range of activity (until an activity of 0.7) for TSDK/BisAF. The second step, concerned with the change in the magnitude of the Fickian and the relaxation contributions to the global mechanism, occurs then at higher activity for TSDK/BisAF than for SDFBP/BisAF. According to these results, it seems that the activity at which the relaxation contribution becomes the major one in the water sorption process is shifted to higher value for TSDK/BisAF in comparison with SDFBP/BisAF, despite a totally similar water uptake of the two membranes as a function of the water activity.

Figure 8c displays the evolution of the two rate constants, k_{R1} and k_{R2}, associated with the relaxation contribution. At low activity, the k_R values remain constant, and no significant differences are evidenced between the two membranes. Then, a decrease of the k_R values is observed. This decrease occurs when the relaxation contribution, Φ_R, increases, which means at an activity close to 0.5 for SDFBP/BisAF and close to 0.7 for TSDK/BisAF.

The detailed analysis of the water sorption mechanism allows clearly underlining that the sorption thermodynamic, and kinetic factors are not sensitive to exactly the same polymer structural parameters. The thermodynamic characteristics, i.e., the isotherm shape and water uptake values, are directly related to the sulfonic group content within the material. The kinetic parameters and especially the parameters characterizing the relaxation contribution to the water sorption mechanism seem to be much more sensitive to the sulfonic acid group location. The relaxation contribution seems to play a predominant role in the water sorption mechanism for the SDFBP/BisAF membrane in comparison with the TSDK/BisAF membrane. One can remark that this first membrane is characterized by a higher value of the glass transition temperature linked to a more homogeneous repartition of the sulfonic acid groups all along the polymer backbone and to smaller ionic clusters dispersed within the material at the nanoscopic scale. It seems then that for SDFBP/BisAF, which is the more rigid system, the relaxation process is required to occur at lower activity to accommodate the water sorption mechanism, allowing finally reaching the same water uptake than in the more flexible TSDK/BisAF.

The gas transport properties, which are of great interest for fuel cell performance and long-term working, were studied for an extended range of gases (helium, hydrogen, and carbon dioxide) and for increasing water content within the membranes with two main goals. The first one was to position the SPAEK gas transport properties with respect to those of Nafion (indeed, only few data concerned with gas transport are reported in the literature for SPEEK and SPAEK) and the second one was to go deeper in the analysis of the role of the sulfonic acid group repartition in the transport mechanisms. Figures 9a and 9b show the evolution of the gas permeability coefficients as a function of the water activity for the SDFBP/BisAF and TSDK/BisAF membranes, respectively.

One can first remark that, at anhydrous state (meaning at water activity equal to 0), the gas permeability values measured on SPAEK are slightly higher than those commonly reported for Nafion.[43,44] Moreover, the permeability coefficients determined on TSDK/BisAF membrane are higher (by a factor around 1.4) than those measured on SDFBP/BisAF membrane. The repartition of the sulfonic acid groups within SPAEK plays in fact a significant role on the kinetic parameter of the transport, as shown by the detailed analysis of the CO_2 transport, for which both diffusion and solubility coefficients can be determined with a good precision. The CO_2 diffusion

coefficient value is lower for the SDFBP/BisAF membrane which presents the more homogeneous repartition of the sulfonated groups than for the TSDK/BisAF membrane ((1.90 ± 0.13) and (2.55 ± 0.20) × 10^{-9} cm^2 s^{-1}, respectively), whereas the solubility coefficient values deduced from the law $P = DS$ are similar ((12.7 ± 1.0) × 10^{-2} cm^3_{STP} cm^{-3} cm_{Hg}^{-1} and (12.1 ± 0.97) × 10^{-2} cm^3_{STP} cm^{-3} cm_{Hg}^{-1}). This behavior is consistent, on one hand, with the higher glass transition temperature value measured on SDFBP/BisAF and, on the other hand, with the models which consider that, in sulfonic acid-based ionomers at anhydrous state, the ionic domains can be considered as low gas permeable domains in comparison with the nonionic phase, due to their high cohesive energy density.[45,46] A more homogeneous dispersion of these low permeable domains within the matrix could then lead to a higher tortuosity effect.

Upon hydration, the SDFBP/BisAF membrane remains lower gas permeable than the TSDK/BisAF membrane, and both membranes become lower gas permeable than Nafion.[44,47] However, the membranes' behavior seems to highly depend on the gas nature. For He and H_2, the gas permeability coefficients first decrease as the water activity increases, then stabilize, and at last slightly increase at activity above 0.8. This last domain could only be observed for SDFBP/BisAF because TSDK/BisAF membranes systematically broke during gas experiment performed at high hydration rate. The flux depressing effect of water at low pressures has already been observed on other low flexible ionomers such as sulfonated polyimides[48] whereas such behavior has not been reported on Nafion,[44,47] for which continuously increasing gas permeability values are generally observed. These data evidence an antiplasticization effect of water in SPAEK, which is in agreement with the high stiffness of the polymer chains. At low activity, the water molecules entering in the film contribute to the formation of the primary hydration shell of the ionic groups and are then in strong interaction with the sulfonic acid groups. However, this first water sorption step involves also the contribution of pre-existing free volumes in the immediate vicinity of the ionic groups which become then no more available for gas diffusion. At higher activity, the additional water uptake is, as previously observed, accompanied by an increasing relaxation diffusion contribution which is related to a polymer chain accommodation toward the sorption mechanism. We can however observe that this phenomenon results in a rather constant gas permeability value. A slight increase of the permeability coefficient is only observed at high water activity. This result shows that the plasticization effects induced by water sorption, which generally lead to huge gas permeability increase, can be considered as very limited in SPAEK. This conclusion is consistent with the observations of Wu et al.,[14] who suggested that water could be sorbed in SPEEK with little change in the bulk volume. The different behavior observed for CO_2, consisting in a constant value of the gas permeability in the activity range between 0 and 0.3 and then a continuous increase of the gas flux as a function of the water activity can be explained by the high affinity of the CO_2 molecules toward water,[43,49] bringing herein a predominant role of an increasing solubility factor in the gas transport mechanism.

4. CONCLUSION

Two sulfonated poly(aryl ether ketone)s having the same ionic exchange capacity but a different sulfonic acid repartition along the polymer backbone were studied. These polymers were synthesized from bisphenol AF, 4,4′-difluorobenzophenone, and either from a classical disulfonated monomer (SDFBP) or from a tetrasulfonated monomer (TSDK). The polymers' thermal properties were investigated by TGA and DSC. The results obtained suggested that the slight chemical structure differences of the two considered SPAEK had a negligible effect on the thermal stability of the membranes. The films were amorphous, and the polymer synthesized from the tetrasulfonated monomer exhibited a lower glass transition temperature compared to that one of the polymer based on the disufonated monomer. The membranes morphology was studied by TEM. Spherical nanometerscale ionic domains were clearly evidenced in both materials, with slightly larger ionic clusters for TSDK/Bis AF.

A detailed analysis of the water and gas transport properties was performed. For water, the coexistence of both Fickian sorption behavior and relaxational phenomena was observed in all the range of water activity, with an increased contribution of relaxation phenomena as the water activity increased. Whatever the diffusing molecule (gas or water vapor), the sulfonic acid groups repartition within the polymer did not affect the solubility values. However, a significant effect was observed on the kinetic parameters. Based on these results, a water sorption mechanism was proposed in relation with the SPAEK architecture, allowing explaining also the evolution of the gas transport properties as a function of hydration rate and gas nature.

AUTHOR INFORMATION

Corresponding Author

*E-mail eliane.espuche@univ-lyon1.fr.

Notes

The authors declare no competing financial interest.

ACKNOWLEDGMENTS

This work has been sponsored by the Agence Nationale de la Recherche (ANR) of France (ANR-07-PANH-002).

REFERENCES

(1) Tang, Y.; Karlsson, A. M.; Santare, M. H.; Gilbert, M.; Cleghorn, S.; Johnson, W. B. *Mater. Sci. Eng.* **2006**, *425*, 297−304.
(2) Majsztrik, P. W.; Bocarsly, A. B.; Benziger, J. B. *Macromolecules* **2008**, *41*, 9849−9862.
(3) Gebel, G.; Aldebert, P.; Pineri, M. *Polymer* **1993**, *34*, 333−339.
(4) Genies, C.; Mercier, R.; Sillion, B.; Cornet, N.; Gebel, G.; Pineri, M. *Polymer* **2001**, *42*, 359−373.
(5) Piroux, F.; Espuche, E.; Mercier, R.; Pineri, M. *J. Membr. Sci.* **2003**, *223* (1−2), 127−139.
(6) Donnadio, A.; Casciola, M.; Di Vona, M. L.; Tamivanan, M. *J. Power Sources* **2012**, *205*, 145−150.
(7) Ohkubo, T.; Ohira, A.; Iwadate, Y. *J. Phys. Chem. Lett.* **2012**, *3* (8), 1030−1034.
(8) Brunetti, A.; Fontananova, E.; Donnadio, A.; Casciola, M.; Di Vona, M. L.; Sgreccia, E.; Drioli, E.; Barbieri, G. *J. Power Sources* **2012**, *205*, 222−230.
(9) Yang, B.; Manthiram, A. *J. Power Sources* **2006**, *153*, 29−35.
(10) Do, K. N. T.; Kim, D. *J. Appl. Polym. Sci.* **2008**, *110*, 1763−1770.
(11) Do, K. N. T.; Kim, D. *J. Power Sources* **2008**, *185*, 63−69.
(12) Zhao, C.; Li, X.; Wang, Z.; Dou, Z.; Zhog, S.; Na, H. *J. Membr. Sci.* **2006**, *280*, 643−650.
(13) Mahajan, C. V.; Ganesan, V. *J. Phys. Chem. B* **2010**, *114*, 8367−8373.
(14) Wu, X.; Wang, X.; He, G.; Benziger. *J. Polym. Sci., Polym. Phys.* **2011**, *49*, 1437−1445.
(15) Shibuya, N.; Porter, R. S. *Macromolecules* **1992**, *25*, 6495−6499.

(16) Xing, P.; Robertson, G. P.; Guiver, M. D.; Mikhailenko, S.; Wang, K.; Kaliaguine, S. *J. Membr. Sci.* **2004**, *229*, 95−106.
(17) Trotta, F.; Drioli, E.; Moraglio, G.; Poma, E. B. *J. Appl. Polym. Sci.* **1998**, *70*, 477−482.
(18) Wang, L.; Meng, Y. Z.; Hay, A. S. *J. Polym. Sci., Part A: Polym. Chem.* **2004**, *42*, 1779−1788.
(19) Bailly, C.; Williams, D. J.; Karasz, F. E.; MacKnight, W. J. *Polymer* **1987**, *28*, 1009−1016.
(20) Zhao, C.; Li, X.; Lin, H.; Shao, K.; Na, H. *J. Appl. Polym. Sci.* **2008**, *108*, 671−680.
(21) Shin, C. K.; Maier, G.; B., A.; Scherer, G. G. *J. Membr. Sci.* **2004**, *245*, 147−161.
(22) Gao, Y.; Robertson, G. P.; Guiver, M. D.; Mikhlailenko, S. D.; Li, X.; Kaliaguine, S. *Macromolecules* **2004**, *37*, 6748−6754.
(23) Shin, C. K.; Maier, G.; Scherer, G. G. *J. Membr. Sci.* **2004**, *245*, 163−173.
(24) Gao, Y.; Robertson, G. P.; Guiver, M. D.; Mikhlailenko, S. D.; Li, X.; Kaliaguine, S. *Macromolecules* **2005**, *38*, 3237−3245.
(25) Wang, F.; Chen, T.; Xu, J.; Liu, T.; Jiang, H.; Qi, Y.; Liu, S.; Li, X. *Polymer* **2006**, *47* (11), 4148−4153.
(26) Kim, D.-S.; Robertson, G. P.; Guiver, M. D.; Lee, Y. M. *J. Membr. Sci.* **2006**, *281*, 111−120.
(27) Wang, F.; Chen, T.; Xu, J. *Macromol. Chem. Phys.* **1998**, *199* (7), 1421−1426.
(28) Khan, A. L.; Li, X.; Vankelecom, I. F. J. *J. Membr. Sci.* **2011**, *372*, 87−96.
(29) Zhao, C.; Lin, Z.; Shao, K.; Li, X.; Ni, H.; Wang, Z.; Na, H. *J. Power Sources* **2006**, *162*, 1003−1009.
(30) Gan, D.; Lu, S.; Wang, Z. *Polym. Int.* **2001**, *50* (7), 812−816.
(31) Knauth, P.; Hou, H.; Bloch, E.; Sgreccia, E.; Di Vona, M. L. *J. Anal. Appl. Pyrolysis* **2011**, *92*, 361−365.
(32) Shashidhara, G. M.; Kumar, K. N. *Polym. Plast. Technol. Eng.* **2010**, *49*, 796−806.
(33) Wilhelm, F. G.; Pünt, I. G. M.; Van Der Vegt, N. F. A.; Strathman, H.; Wessling, M. *J. Membr. Sci.* **2002**, *199* (1−2), 167−176.
(34) Zaidi, S. M. J.; Mikhailenko, S. D.; Robertson, G. P.; Guiver, M. D.; Kaliaguine, S. *J. Membr. Sci.* **2000**, *173*, 17−34.
(35) Gan, D.; Lu, S.; Wang, Z. *Polym. Int.* **2001**, *50* (7), 812−816.
(36) Li, X.; Zhao, C.; Lu, H.; Wang, Z.; Na, H. *Polymer* **2005**, *46*, 5820−5827.
(37) Zhang, H.; Pang, J.; Wang, D.; Li, A.; Li, X.; Ji, Z. *J. Membr. Sci.* **2005**, *264*, 56−64.
(38) Wang, Z.; Li, X.; Zhao, C.; Ni, H.; Na, H. *J. Power Sources* **2006**, *160* (2), 969−976.
(39) Gil, M.; Ji, X.; Na, H.; Hampsey, J. E.; Lu, Y. *J. Membr. Sci.* **2004**, *234*, 75−81.
(40) Potreck, J.; Uyar, F.; Sijbesma, H.; Nijmeijer, K.; Stamatialis, D.; Wessling, M. *Phys. Chem. Chem. Phys.* **2009**, *11*, 298−308.
(41) Despond, S.; Espuche, E.; Cartier, N.; Domard, A. *J. Polym. Sci., Polym. Phys.* **2005**, *43* (1), 48−58.
(42) Berens, A. R.; Hopfenberg, H. B. *Polymer* **1978**, *19*, 489−496.
(43) Ma, S.; Odgaard, M.; Skou, E. *Solid State Ionics* **2005**, *176*, 2923−2927.
(44) Dorenbos, G.; Morohoshi, K. *J. Chem. Phys.* **2011**, *134*, 044133.
(45) Ogumi, Z.; Kuroe, T.; Takehara, Z. *J. Electrochem. Soc.* **1985**, *132*, 2601−2605.
(46) Chiou, J. S.; Paul, D. R. *Ind. Eng. Chem. Res.* **1988**, *27*, 2161−2166.
(47) Broka, K.; Ekdunge, P. *J. Appl. Electrochem.* **1997**, *27*, 117−123.
(48) Piroux, F.; Espuche, E.; Mercier, R. *J. Membr. Sci.* **2004**, *232* (1−2), 115−122.
(49) Despond, S.; Espuche, E.; Domard, A. *J. Polym. Sci., Polym. Phys.* **2001**, *39*, 3114−3127.